AMERICAN JOURNAL OF PHARMTECH RESEARCH

Journal home page: http://www.ajptr.com/

Carbopol® and Chitosan Coated Nanoparticles with *In-Situ* Loaded Indomethacin

Velichka Andonova,[1*] George Georgiev,[2] Vencislava Toncheva,[2] Daniela Karashanova,[3] Plamen Katsarov,[1] Margarita Kassarova[1]

1.Department of Pharmaceutical Sciences, Faculty of Pharmacy, Medical University Plovdiv, Plovdiv, Bulgaria

2.Faculty of Chemistry and Pharmacy, Sofia University "St. Kliment Ohridski", Sofia, Bulgaria

3. Institute of Optical Materials and Technologies "Acad. Jordan Malinovski", Bulgarian Academy of Sciences, Sofia, Bulgaria

ABSTRACT

Indomethacin-loaded nanoparticles (IMC-NPs) were obtained by emulsifier-free radical polymerization of vinyl acetate (VAc) in the presence of indomethacin (IMC) in the aqueous solution of Carbopol® (Cbp) or chitozan (CH). The purpose of this study was to investigate the influence of nature and quantity of the added to the reaction system polymer on IMC loading and its kinetic release properties in terms of the future development of topical ophthalmic formulations. CH was chosen as a cationic polysaccharide and Cbp as an anionic crosslinked polymer. TEM and DLS were used to observe the morphology and to determine the average particle size which was in the range of 178.20÷297.90 nm and the polydispersity index (PDI) which was within 0.149÷0.339. A monomodal particle size distribution (PSD) was observed for the CH-coated NPs and bimodal PSD was observed in the models, obtained in the presence of Cbp. FTIR analysis showed that the models were a result of interactions with hydrogen bonds. UV-spectroscopy was used for the determination of IMC inclusion and *in vitro* release characteristics. The results of release kinetic analyses showed that IMC was released from the investigated models following the first order. The polymer shell (Cbp or CH) around the pVAc–core had an impact on the rate and degree of the released drug.

Keywords: Indomethacin-loaded nanoparticles, radical polymerization, polymer coated nanoparticles, carbopol coated nanoparticles, homopolymers of vinyl(acetate)

*Corresponding Author Email: andonova_v@abv.bg

Received 23 December 2013, Accepted 09 January 2014

Please cite this article in press as: Andonova V.*et al.*, Carbopol® and Chitosan Coated Nanoparticles with *In-Situ* Loaded Indomethacin. American Journal of PharmTech Research 2014.

INTRODUCTION

Indomethacin (IMC), ([1-(4-chlorobenzoyl)-5-methoxy-2-methylindol-3-yl] acetic acid) is a typical nonsteroidal anti-inflammatory agent (NSAIA) which also has analgesic and antipyretic activity and it is used to treat osteoarthritis, rheumatoid arthritis, bursitis, tendinitis, gout, ankylosing spondylitis and headaches[1]. IMC may cause serious adverse effects and should not be used simply as an analgesic or antipyretic drug[1]. Indomethacin is a poorly soluble, highly permeable (Class II) drug, its oral absorption is often controlled by the dissolution rate in the gastrointestinal tract[2]. Due to its insolubility in water, the drug formulations, in which it is included, often show low and erratic bioavailability and the oral administration causes stronger irritation of the stomach lining due to the prolonged contact with it[3, 4]. In ophthalmology IMC is used in topical eye drops for prevention of miosis during cataract surgery, cystoid macular edema and conjunctivitis[1, 5]. Its use in liquid formulations is limited due to insolubility in water, low bioavailability and ocular mucosa irritation.

In the last decade researches define the use of NPs with biocompatible and biodegradable polymers as effective drug-release systems, which aim is to increase the solubility and bioavailability and reduce the irritating effects of the drugs[6]. In order to overcome the technological problems, associated with the insolubility and instability of IMC in the aqueous medium and its low bioavailability after a topical application (for ophthalmic formulations), various models of drug-delivery systems have been developed. IMC has been included into nanosuspensions[7-9], microemulsions[7, 10], polymeric NPs[6, 11, 12]. Different methods and a huge variety of excipients have been used to increase the solubility and bioavailability and reduce the side effects of the drug. For example, NPs based on copolymers of methyl methacrylate and glycidyl methacrylate with IMC have been developed via emulsion radical polymerization [11]. Other studies have been made on NPs of cyclodextrin with IMC [12]. Kumar et al. have conducted *in vitro* and *in vivo* study of IMC loaded gelatine NPs [13]. They have prepared the NPs by a double desolvation method for controlled drug delivery. IMC loaded gelatine NPs with a good *in vitro-in vivo* correlation have established the formulation for future trials. Liu et al. have used the anionic polymerization procedure to obtain IMC loaded poly(butylcyanoacrylate) NPs[14]. *In vitro* drug release has revealed that IMC incorporation and/or adsorption leeds to a rapid drug release which is followed by a slower release in a biological phosphate buffer and that the release rate decreases with the increase of the IMC content in the particle. In another study Tomoda et al. have observed enhanced transdermal delivery of IMC loaded PLGA NPs by iontophoresis[15].

On the other hand pVAc emulsion homopolymer and VAc based emulsion copolymers are of great importance in an industrial and scientific aspect[16-18]. In our previous study we have demonstrated the possibility of *in-situ* inclusion of IMC in pVAc and polystyrene NPs using emulsifier-free radical polymerization of monomers[19] and have determined the best conditions for this process[20].

It is known from the literature that the addition of a solution of a polymer to the reaction system affects the NPs morphology and the drug release properties. This effect can be determined by the type of monomers which are used in the polymerization process, the physicochemical properties of the polymer, and last but not least by the properties of the used drug. According to many authors, coating of the NPs with a suitable polymer leads to a change in the release kinetic properties and may reduce or prevent burst release, or reduce the side effects of certain drugs[21-23].

The purpose of this study is to investigate the influence of nature and quantity of the added to the reaction system polymer on IMC loading and its kinetic release properties in terms of future development of topical ophthalmic formulations. Both polymers Cbp and CH have been chosen mainly due to their mucoadhesive and penetration-enhancing properties[24, 25]. CH is a cationic polysaccharide and Cbp is an anionic crosslinked polymer. They also have a good biocompatibility with ocular structures[25].

MATERIALS AND METHOD

Materials

In this research IMC as a drug and vinyl acetate (VAc) as a monomer were purchased from Fluka. Potassium dihydrogen phosphate and *di*-sodium hydrogen phosphate from Merck (Darmstadt, Germany) were used for the preparation of a phosphate-phosphate buffer (Sorensen's phosphate buffer) (PPB). Ammonium persulfate (AP) (Fluka) was used as an initiator. Carbopol 971 (BF Goodrich, Cleveland, OH) and chitosan (medium molecular weight) (Fluka) were used as polymers for the preparation of IMC-NPs.

Preparation of IMC-loaded nanocarriers

IMC-loaded nanoparticles (IMC-NPs) were obtained by emulsifier-free radical polymerization of VAc monomers 10% (v/v), in the presence of IMC 1% (w/v) in the aqueous solution of Cbp or CH in different mass ratio: (i) VAc:Cbp = 10:1 and Cbp:IMC = 1:1; (ii) VAc:Cbp = 20:1 and Cbp:IMC = 1:2; (iii) VAc:CH = 10:1 and CH:IMC = 1:1; (iv) VAc:CH = 20:1 and CH:IMC = 1:2. The polymerization was conducted in a nitrogen atmosphere and temperature of 55°C, for 90

min under ultrasound impact (Ultrasonicator Siel UST7.8-200, Gabrovo, Bulgaria). Ammonium persulphate (AP) in concentration 1% (w/v) was used as an initiator. The model latex was exposed to dialysis through membrane with MWCO 8000 Da for 7 h for elimination of compounds with low molecular weight (e.g. the initiator, residual monomers or free IMC) from the primary latex[19, 20].

Transmission Electron Microscopy

TEM images of the investigated models were carried out by transmission electron microscope JEOL JEM 2100 (JEOL Ltd., Japan) with accelerating voltage 200 kV. Before the samples were observed under the microscope, the following preparation had been made: micro-quantities of the studied substance were mixed with distilled water into a test tube and placed in an ultrasonic bath to homogenise for 3 min. Thereafter the suspension was dropped on carbon-coated standard Cu grid and dried under air conditions in a dust free environment for 24 h.

Particle size distribution and zeta potential analysis

Particle size distribution (PSD) of the NPs was determined by dynamic light scattering (DLS, Zetasizer Nano ZS, Malvern Instruments, Malvern, UK) in measurement range of 0.3 nm – 10 µm (diameter), minimum sample volume 12 µl. The samples were prepared using equal quantity of NPs in a phosphate–phosphate buffer at pH 7.4 (Sorensen's phosphate buffer) (PPB) and were filtered through a filter Chromafil Xtra 0.45 µm before measuring the particle mean diameter and PDI. Zeta potential **(**ZP) of NPs was also measured under the same conditions using the principle of electrophoretic light scattering with the same apparatus Zetasizer Nano ZS with specifications: light source He-Ne laser 632.8 nm, 4 mW and backscatter detection at 173°. The experiments were repeated three times and the results were calculated as mean values.

Fourier Transform Infrared spectroscopic analysis

Fourier Transform Infrared spectroscopic analysis (FTIR) was carried out with FTIR Bruker Tensor 37 Spectrometer (Bruker Optics GmbH, Germany), using the technique of tableting with KBr and resolution 2 cm^{-1} at 120 scans for each sample.

Drug loading assessment

To determine the amount of incorporated IMC into the NPs, 2.5 mg of IMC loaded NPs were weighed and dissolved into 25.0 ml methanol and placed under ultrasound impact (Ultrasonicator Siel UST7.8-200, Gabrovo, Bulgaria) for 90 min.The quantitative defining of IMC was made spectrophotometrically at λ=320 nm with UV/VIS spectrophotometer Ultrospec 3300 (Biochrom Ltd., Cambridge, UK) after filtering the samples through a filter Chromafil Xtra 0.45 µm. Control experiments were performed for any absorbance using blank NPs without IMC.

The measurements were made compared to the examination medium. The total drug content of each formulation was calculated from the standard curve (with a linearity coefficient (r) = 0.999). Each experiment was repeated six times and the results were presented as means ± SD. The drug loading (%DL), encapsulation efficiency (%EE) and NPs yield (%Y) were calculated using the following equations:

$$\%DL = \frac{\text{Weight of IMC entrapped within NPs}}{\text{Total weigh of NPs}} \text{x}100 \quad (1)$$

$$\%EE = \frac{\text{Weight of IMC entrapped within NPs}}{\text{Total IMC added}} \text{x}100 \quad (2)$$

$$\%Y = \frac{\text{Total weigh of NPs}}{\text{Weight of polymer +weigh of IMC}} \text{x}100 \quad (3)$$

***In vitro* release study of IMC from nanocarriers**

Examination of the release of IMC from the model nanosized particles was carried out in a thermostated vessel with equal amounts of the tested models under perfect "sink" conditions; working volume for dissolution 100.0 ml PPB at pH 7.4; temperature 37°C±0.5°C; stirring speed 100 min^{-1}. The quantitative defining of IMC was made spectrophotometrically at λ=320 nm with UV/VIS spectrophotometer Ultrospec 3300 pro (Biochrom Ltd., Cambridge, UK) after filtering the samples through a filter Chromafil Xtra 0.45 μm. The measurements were made compared to the examination medium Sorensen's PPB at pH 7.4. Control experiments were performed using NPs without IMC. The experiments were repeated six times, the results were presented as mean values and the concentrations were calculated from the standard curve with a linearity coefficient (r) = 0.999.

RESULTS AND DISCUSION

Obtaining of IMC-loaded nanocarriers

IMC-loaded nanoparticles (IMC-NPs) were obtained by emulsifier-free radical polymerization of VAc monomers 10% (v/v), in the presence of IMC 1% (w/v) in the aqueous solution of Cbp or CH in different mass ratio (Table 1). The used Cbp is lightly crosslinked polymer and the most efficient grade for controlling drug release. Due to the anionic nature of the Cbp there is a pH-dependence: at lower pH values the polymer is not fully swollen and there are larger regions of microviscosity. When pH is increased, the ionization of the carboxylic acid groups causes maximum swelling, resulting in fewer and smaller regions of microviscosity. The gel formation acts as a barrier for the release of the drug[23, 24]. Contrariwise, CH is a linear polysaccharide,

composed of randomly distributed β-(1-4)-linked D-glucosamine (deacetylated) and N-acetyl-D-glucosamine (acetylated) units. The amino group in CH has a pKa value of ~6.5, which leads to protonation in an acidic to neutral solution with a charge density, which is dependent on pH-value. This is very important for the biomedical applications. This molecule will maintain its structure in a neutral environment, but it will solubilize and degrade in an acidic environment. This makes CH water soluble and bioadhesive - it readily binds to negatively charged surfaces such as mucosal membranes[6, 24, 25].

Table 1: Investigated models. Type and concentration of the aqueous solution of the polymer, which was used for their obtaining

Model	Type and concentration of the solution
IMC-p(VAc)+Cbp-1	An aqueous solution of Cbp 1% (w/v) (in mass ratio VAc:Cbp = 10:1 and Cbp:IMC=1:1).
IMC-p(VAc)+Cbp-2	An aqueous solution of Cbp 0.5% (w/v) (in mass ratio VAc:Cbp = 20:1 and Cbp:IMC=1:2).
IMC-p(VAc)+CH-1	An aqueous solution of CH 1% (w/v) (in mass ratio VAc:CH = 10:1 and CH:IMC=1:1).
IMC-p(VAc)+CH-2	An aqueous solution of CH 0.5% (w/v) (in mass ratio VAc:CH = 20:1 and CH:IMC=1:2).

Table 2: Zeta potential (ZP), polydispersity index (PDI), average particle size (Z-average) and particle size distribution (PSD) of IMC-p(VAc)+Cbp-1, IMC-p(VAc)+Cbp-2, IMC-p(VAc)+CH-1, and IMC-p(VAc)+CH-2

Model	ZP, [mV]	PDI	Z-average, [nm]	PSD *Peak 1, [nm]*	*Peak 2, [nm]*	*Area 1, [%]*	*Area 2, [%]*
IMC-p(VAc)+Cbp-1	-31.5	0.224	197.5	213.6	34.55	94.56	5.44
IMC-p(VAc)+Cbp-2	-29.5	0.287	178.2	235	47.5	90.5	9.5
IMC-p(VAc)+CH-1	-0.437	0.149	260.8	260.8	-	100	-
IMC-p(VAc)+CH-2	67.4% NPs with 9 and 32.6% with (-33)	0.339	297.9	297.9	-	100	-

Transmission Electron Microscopy imaging of NPs

Figure 1 shows the TEM images of IMC-p(VAc)+Cbp-1 (Figure 1a), IMC-p(VAc)+Cbp-2 (Figure 1b), IMC-p(VAc)+CH-1 (Figure 1c) and IMC-p(VAc)+CH-2 (Figure 1d). The observed models had an oval shape and approximately same dimensions (400-600 nm). The particles had a porous structure (Figures 1a, c, d). Very small particles were observed in all of the models. This result had an impact on the particle size distribution. Figure 1c shows the CH-layer around the

IMC-pVAc-core in IMC-p(VAc)-CH-1 model. This CH-layer was not observed in IMC-p(VAc)-CH-2 as clearly as in IMC-p(VAc)-CH-1 model. A possible reason for this could be the two times smaller quantity of CH, used during the obtaining of IMC-p(VAc)+CH-2. Generally, the difference in the polymer concentration did not affect the morphology and the size of the NPs.

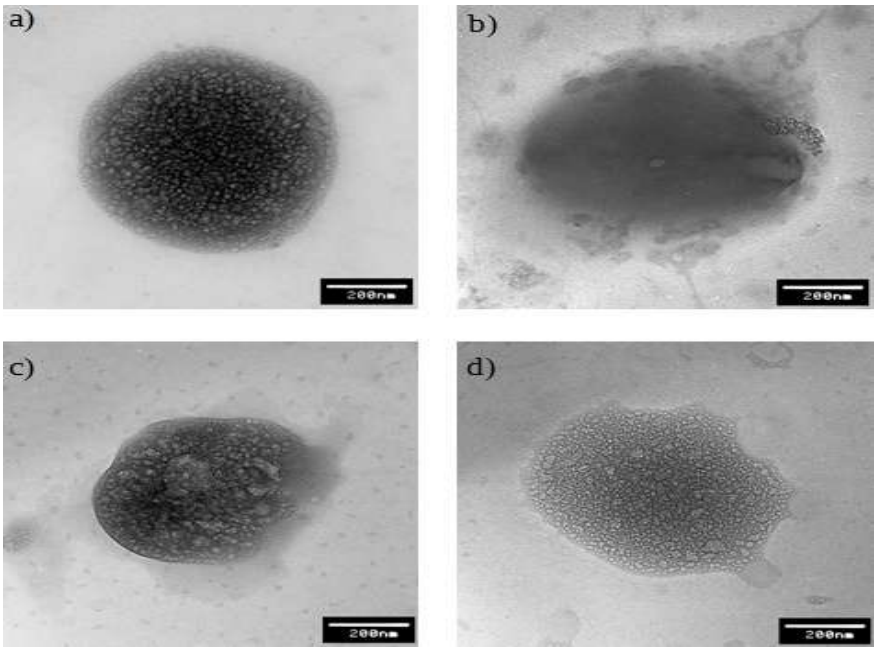

Figure 1: TEM images of IMC-p(VAc)+Cbp-1 (a), IMC-p(VAc)+Cbp-2 (b), IMC-p(VAc)+CH-1 (c), and IMC-p(VAc)+CH-2 (d).

Particle size distribution and zeta potential assessments

The results of the PSD and ZP analyzes are presented in Table 2. The data showed that the models coated with Cbp had similar values of ZP and average particle size (z-average). In these patterns was observed bimodal PSD which could be explained by obtaining of two types of NPs: a group of Cbp-coated NPs in area 1 and another group of uncoated NPs in area 2. Uncoated NPs increased with decreasing of used Cbp in model IMC-p(VAc)+Cbp-2. CH-coated NPs had a monomodal PSD and acceptable values of PDI. IMC-p(VAc)+CH-1 was composed of NPs with low value of ZP (-0.437 mV), which could be explained by the cationic nature of CH. It neutralized the negatively charged groups of IMC and VAc-monomers, regardless of the mass ratio VAc:CH = 10:1 and CH:IMC = 1:1. But absolute values of ZP over 30 mV are the criteria for relative physical stability of the system[26, 27] and if ZP is lower (in model IMC-p(VAc)+CH-1) the possibility of aggregation among the particles is larger. An interesting fact was the bimodal distribution of ZP in model IMC-p(VAc)+CH-2: 67.4% of the NPs were positively (average 9.49 mV) and 32.6% were negatively charged (average -33 mV). This result could be explained similarly by the obtaining of two types of NPs: a group of CH coated NPs and a second group of

uncoated NPs. It was probably because of the two times smaller quantity of CH in IMC-p(VAc)+CH-2 compared to IMC-p(VAc)+CH-1. The CH shell around the NPs was very thin and its lack did not affect PSD modality as in Cbp-coated NPs.

Adding Cbp in the polymerization system led to the obtaining of NPs with bimodal PSD (Cbp-coated and uncoated NPs) and acceptable ZP values. The inclusion of cationic polymer CH in the polymerization mixture led to the obtaining of NPs with monomodal PSD and bimodal distribution of ZP only for model IMC-p(VAc)+CH-2. With the best performance in terms of z-average, PDI and ZP (as a measure of physical stability of the systems) were IMC-p(VAc)+Cbp-1 and IMC-p(VAc)+Cbp-2.

Fourier Transform Infrared spectroscopic analysis

Figure 2 shows the IR-spectra of the investigated models IMC-p(VAc)+Cbp-1 and IMC-p(VAc)+Cbp-2 compared to the spectra of p(VAc)+Cbp-1 (NPs without IMC, obtained in the presence of 1% Cbp) and pure IMC. In the spectrum of pure IMC (γ – type, more stable and less soluble polymorph modification of IMC in comparison with α - modification) are shown the two most intensive peaks at 1717 cm^{-1} and at 1690 cm^{-1} of υC=O[9, 28]. The spectra of the tested models showed a similarity with these of pure IMC. Obviously the systems were not a chemical interaction between the polymer and IMC but rather a result of interactions with weak hydrogen bonds[9, 23, 28].

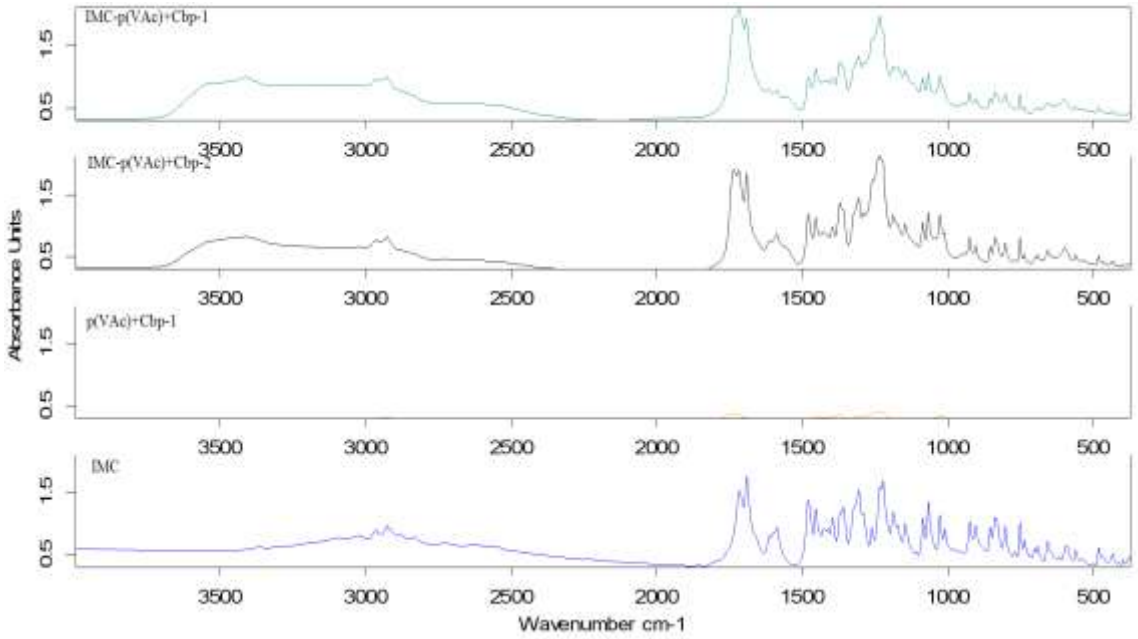

Figure 2: FTIR-spectra of IMC-p(VAc)+Cbp-1, IMC-p(VAc)+Cbp-2, p(VAc)+Cbp-1 (NPs without IMC, obtained in the presence of 1% Cbp), and IMC.

Figure 3 shows the IR-spectra of the investigated models IMC-p(VAc)+CH-1 and IMC-p(VAc)+CH-2 compared to the spectra of p(VAc)+CH-1 (NPs without IMC, obtained in the presence of 1% Cbp) and pure IMC. In IMC-p(VAc)+CH-1 and IMC-p(VAc)+CH-2 (Figure 3) we see the characteristic absorption peaks, but the spectra are less similar to these of pure IMC in comparison with the Cbp-coated models. A possible reason for this may be the smaller quantity of incorporated IMC into the NPs.

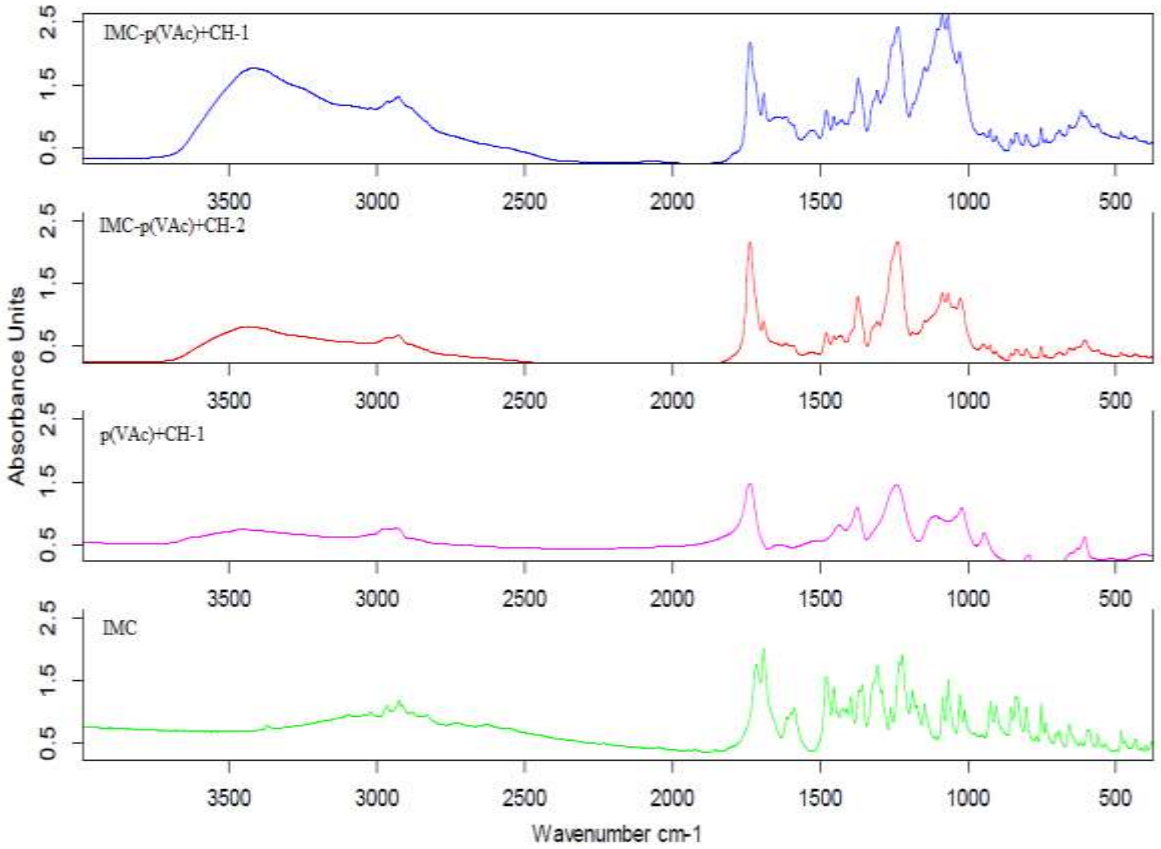

Figure 3: FTIR-spectra of IMC-p(VAc)+CH-1, IMC-p(VAc)+CH-2, p(VAc)+CH-1 (NPs without IMC, obtained in the presence of 1% CH), and IMC.

Drug loading assessment

The investigation of IMC loading in the NPs is presented in Table 3. The data show higher values in the Cbp-coated model compared to CH-coated NPs probably due to the difference in their nature. The values in IMC-p(VAc)+Cbp-2 and IMC-p(VAc)+CH-2 are higher than those in IMC-p(VAc)+Cbp-1 and IMC-p(VAc)+CH-1. A possible reason for this could be the higher viscosity of the aqueous solutions of Cbp and CH in 1% concentration, compared to the same solutions in 0.5%. The higher concentration of the polymer in aqueous medium hampers NPs formation and %Y, %EE and %DL are lower than those of IMC-p(VAc)+Cbp-2 and IMC-p(VAc)+CH-2.

Table 3: Encapsulation efficiency (%EE), drug loading (%DL), and NPs yield (%Y)

Model	%EE±SD	%DL±SD	%Y±SD
IMC-p(VAc)+Cbp-1	47.56±0.51	5.21±0.32	88.32±1.33
IMC-p(VAc)+Cbp-2	48.82±0.77	5.30±0.65	89.02±1.09
IMC-p(VAc)+CH-1	29.87±0.45	3.34±0.23	85.87±0.98
IMC-p(VAc)+CH-2	34.03±0.84	3.85±0.54	86.45±1.45

**SD – standard deviation, n=6*

***In vitro* study of IMC release from nanocarriers**

Figure 4 presents the profiles of IMC release from the carriers IMC-p(VAc)+Cbp-1, IMC-p(VAc)+Cbp-2, IMC-p(VAc)+CH-1 and IMC-p(VAc)+CH-2. Blank formulations did not have any significant absorbance at 320 nm. The study was conducted for 16 h.

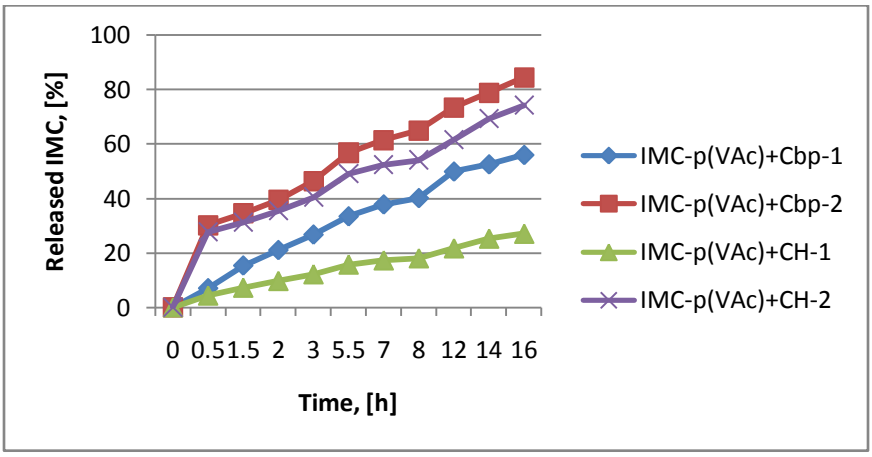

Figure 4: Profiles of released IMC from models IMC-p(VAc)+Cbp-1, IMC-p(VAc)+Cbp-2, IMC-p(VAc)+CH-1, and IMC-p(VAc)+CH-2.

The comparison between the release profile of IMC from IMC-p(VAc)+Cbp-1 and that from IMC-p(VAc)+Cbp-2 showed that the model IMC-p(VAc)+Cbp-2 released at any moment higher amount of IMC. At the end of the study 84.33% of the included IMC was released from IMC-p(VAc)+Cbp-2 compared to model IMC-p(VAc)+Cbp-1, which released only 55.98% of the included drug. The difference in the rate and the degree of IMC release from both Cbp-coated models was due to the smaller quantity of Cbp in model IMC-p(VAc)+Cbp-2, which had enclosed the particles. The two times bigger amount of Cbp in model IMC-p(VAc)+Cbp-1 led to the formation of a thicker Cbp shell around the particles. That shell limited the rate and the degree of the release of included IMC: wetting and swelling of Cbp, penetration of water into the pores of the core, eluting of IMC included in these pores and the diffusion of the drug through the gel layer of Cbp. Model IMC-p(VAc)+Cbp-1 released IMC according to the following equation

$$c = -0{,}175 \times t^2 + 7{,}689 \times t - 7{,}193, [\%] \qquad (4)$$

$$R^2 = 0{,}995$$

Where "c" is the concentration of released IMC in % and "t" is the time of its release in hour. IMC-p(VAc)+Cbp-2 model released 30% of the included IMC for half an hour and then the remaining amount of the drug was released with sufficient accuracy according the equation:

$$c = -0{,}021 \times t^2 + 6{,}460 \times t + 22{,}26, [\%] \quad (5)$$

$$R^2 = 0{,}993$$

A similar dependence was observed in the models IMC-p(VAc)+CH-1 and IMC-p(VAc)+CH-2. IMC-p(VAc)+CH-2 released approximately three times more IMC compared to IMC-p(VAc)+CH-1 for the same period of time. Model IMC-p(VAc)+CH-1 released IMC following the equation:

$$c = -0{,}04 \times t^2 + 3{,}070 \times t - 2{,}133, [\%] \quad (6)$$

$$R^2 = 0{,}991.$$

Model IMC-p(VAc)+CH-2, similarly to IMC-p(VAc)+Cbp-2, released 28% of the included IMC after half an hour and the remaining amount of the drug was released according to the equation:

$$c = 0{,}099 \times t^2 + 4{,}119 \times t + 23{,}10, [\%] \quad (7)$$

$$R^2 = 0{,}991.$$

This two-step release in models IMC-p(VAc)+Cbp-2 and IMC-p(VAc)+CH-2 could be explained with the release of IMC located on the pVAc-surface of the uncoated NPs.

All investigated models demonstrated a sustained release of the included IMC within 16 hour[9, 23]. There was a similarity between the release kinetics of the included IMC in the models obtained in an analogous manner: IMC-p(VAc)+Cbp-1 and IMC-p(VAc)+CH-1 and also the pair IMC-p(VAc)+Cbp-2 and IMC-p(VAc)+CH-2. Among the tested models the largest amount of released IMC was seen in model IMC-p(VAc)+Cbp-2.

To determine the kinetic models that describe the best the release mechanism, the *in vitro* release data were analyzed according to zero-, first-order and Higuchi model. The model with the highest correlation coefficient (R^2) was selected as the best fit[21]. The results showed that IMC was released from all investigated patterns following the first order kinetics (Table 4). These results relate to conditions in which there is no change in the shape of the NPs during the dissolution process (i.e. the surface area remains constant)[29]. This result can be explained by the hydrophobic nature of the pVAc-core and the included IMC. Cbp- or CH-shell limits the rate and the degree of IMC-release but does not affect the kinetic model and the drug transport mechanism. Perhaps this shell is very thin and it does not change during the exploration. Based

on the higher values of R^2 according to Higuchi model we can determine the drug transport mechanism as Fickian diffusion[30].

Table 4: Correlation coefficient (R^2) of different kinetic models for IMC-NPs

Formulation	Correlation coefficient (R^2)			Drug transport mechanism
	Zero	*First*	*Higuchi*	
IMC-p(VAc)+Cbp-1	0,902	0,993	0,988	Fickian diffusion
IMC-p(VAc)+Cbp-2	0,819	0,970	0,939	Fickian diffusion
IMC-p(VAc)+CH-1	0,920	0,991	0,989	Fickian diffusion
IMC-p(VAc)+CH-2	0,816	0,961	0,928	Fickian diffusion

CONCLUSION

There was no data in the literature about the interaction between IMC and the used monomers and between the initiator of the polymerization and IMC, as well as about the IMC influence on the stability of the monomer and polymer dispersions in water. The preliminary experiments allowed choosing the emulsion polymerization conditions, excluding chemical modification and degradation of the IMC molecule[19, 20]. On the other hand, the IMC concentration (1% (w/v)) led to minimum coagulate formations during the polymerization with high yield of NPs (Table 3). Even more, stable polymer latexes with included IMC in nanosized particles were produced without the usage of surfactants - an important advantage of this method for a drug formulation. The challenge was to find easily available and feasible technological parameters for the effective control of the IMC release from the polymer NPs. This control was achieved by changes in the composition of the polymer mixture (pVA, Cbp and CH) from which the NPs with included IMC were prepared. For that purpose IMC-NPs were produced by emulsifier-free radical polymerization of VAc monomers 10% (v/v), in the presence of IMC 1% (w/v) in the aqueous solution of Cbp or CH in different mass ratio. The obtained results confirmed the efficiency of this approach for the control of the IMC degree of loading, encapsulation efficiency, its release degree and rate. The difference in the concentration in aqueous solutions of Cbp did not affect the structure and the size of Cbp-coated NPs. Regardless of the concentration of added Cbp, NPs were obtained with bimodal PSD and acceptable values of ZP in terms of moderate system stability. The inclusion of the cationic polymer CH in the polymerization mixture led to the obtaining of NPs with monomodal PSD and bimodal distribution of ZP only for model IMC-p(VAc)+CH-2, connected with two times smaller amount of CH in this model. The current Cbp- and CH-coated carriers were not a chemical interaction between the polymer and IMC but rather a result from interactions with weak hydrogen bonds. Higher values of %Y, %EE and %DL were observed for the Cbp-coated model compared to the CH-coated NPs due to the difference in their

nature. These values were higher in the models obtained with two times smaller quantity of added polymer. Investigated models demonstrated a sustained release of the included IMC within 16 hours following the first order release kinetic. According to the current research IMC-p(VAc)+Cbp-2 was the most promising model in terms of the future development of topical ophthalmic formulations.

ACKNOWLEDGMENTS

The authors are grateful to the National Science Foundation (Project DDVU-02/43) and to Medical University of Plovdiv (Project HO-13/2013) for the financial support.

REFERENCES:

1. Sweetman SC. Martindale: The complete drug reference, 33 ed., London Pharmaceutical Press; 2007.
2. Lobenberg R, Amidon GL. Modern bioavailability, bioequivalence and biopharmaceutics classification system; new scientific approaches to international regulatory standards. Eur J Pharm Biopharm 2000; 50: 3–12.
3. Hirasawa N, Ishise S, Miyata H, Danjo K. Physicochemical characterization and drug release studies of nilvadipine solid dispersions using water-insoluble polymer as a carrier. Drug Dev Ind Pharm 2003; 29: 339-44.
4. Alsaidan SM, Alsughayer AA, Eshra AG. Improved dissolution rate of indomethacin by adsorbents. Drug Dev Ind Pharm 1998; 24: 389-94.
5. Wickstrom K. Acute bacterial conjunctivitis - benefits versus risks with antibiotic treatment. Acta Ophthalmol (Oxf) 2008; 86: 2–4.
6. Motwani SK, Chopra S, Talegaonkar S, Kohli K, Ahmad FJ, Khar RK. Chitosan - sodium alginate nanoparticles as submicroscopic reservoirs for ocular delivery: Formulation, optimisation and in vitro characterization. Eur J Pharm Biopharm 2008; 68: 513–25.
7. Calvo P, Vila-Jato JL, Alonso MJ. Comparative *in vitro* evaluation of several colloidal systems, nanoparticles, nanocapsules and nanoemulsions as ocular drug carriers. J Pharm Sci 1996; 85: 530–6.
8. Vulovic N, Primorac M, Stupar M, and Ford JL. Some studies into the properties of indomethacin suspensions intended for ophthalmic use. Int J Pharm 1989; 55: 123–8.
9. Mokarram RA, Kebriaeezadeh A, Keshavarz M, Ahmadi A, Mohtat B. Preparation and in-vitro evaluation of indomethacin nanoparticles. DARU. 2010; 18(3).

10. Muchtar S, Abdulrazik M, Frucht-Pery J, and Benita S. Ex vivo permeation study of indomethacin from a submicron emulsion through albino rabbit cornea. J Control Release 1997; 44: 55.
11. Nita LE, Chiriac AP, Nistor M. An in vitro release study of indomethacin from nanoparticles based on methyl methacrylate/glycidyl methacrylate copolymers. J Mater Sci: Mater Med. 2010; 21: 3129-40.
12. Wongmekiat A, Yoshimatsu S, Tozuka Y, Moribe K, Yamamoto K. Investigation of drug Nanoparticulate Formation by Co-grinding with Ciclodextrins: Studies for Indometacin, Furosemide and Naproxen. J Incl Phenom Macro 2006; 56: 29-32.
13. Kumar R, Nagarwal RC, Dhanawat M, Pandit JK. In-vitro and in-vivo study of indomethacin loaded gelatin nanoparticles. J Biomed Nanotechnol 2011; 7(3): 325-33.
14. Liu H, Chen J. Indomethacin-loaded poly(butylcyanoacrylate) nanoparticles: preparation and characterization. PDA J Pharm Sci Technol 2009; 63(3): 207-16.
15. Tomoda K, Terashima H, Suzuki K, Inagi T, Terada H, Makino K. Enhanced transdermal delivery of indomethacin-loaded PLGA nanoparticles by iontophoresis. Colloids Surf B Biointerfaces. 2011; 88(2): 706-10.
16. Yamak HB. Emulsion Polymerization: Effects of Polymerization Variables on the Properties of Vinyl Acetate Based Emulsion Polymers, Polymer Science, Dr. Faris Yılmaz (Ed.), ISBN: 978-953-51-0941-9, InTech, 2013; DOI: 10.5772/51498.
17. Herk A. Chemistry and Technology of Emulsion Polymerization. Oxford: Blackwell Publishing; 2005.
18. Chern CS. Emulsion Polymerization Mechanisms and Kinetics. Prog Polym Sci 2006; 31: 443-86.
19. Andonova V, Georgiev G, Toncheva V, Kassarova M. Preparation and study of poly(vinyl acetate) and poly(styrene) nanosized latex with indometacin. Pharmazie. 2012; 67(7): 601-4.
20. Andonova V, Georgiev G, Toncheva V, Petrova N, Kassarova M. Nanoparticles with indometacin – drug delivery systems for ocular administration. Folia Medica. 2013; 55(1): 76-82.
21. Ibrahim MM, Abd-Elgawad HAE, Soliman OAE, Jablonski M. Natural bioadhesive biodegradable nanoparticles - based topical ophthalmic formulations for sustained celecoxib release: In vitro Study. JPTDR. 2013;

22. Budhian A, Siegel SJ, Winey KI. Controlling the in vitro release profiles for a system of haloperidol-loaded PLGA nanoparticles. Int J Pharm 2008; 346: 151-9.
23. Tzankov B, Yoncheva K, Popova M, Szegedi A, Momekov G, Mihaly J, Lambov N. Indometacin loading and in vitro release properties from novel carbopol coated spherical mesoporous silica nanoparticles. Micropor Mesopor Mat 2013; 171: 131-8.
24. Ludwig A. The use of mucoadhesive polymers in ocular drug delivery. Adv Drug Delivery Rev 2005; 57: 1595-1639.
25. de la Fuente M, Raviña M, Paolicelli P, Sanchez A, Seijo B, Alonso MJ. Chitosan-based nanostructures: A delivery platform for ocular therapeutics, Adv Drug Delivery Rev 2010; 62(1): 100-17.
26. Nagarwal RC, Kant S, Singh PN, Maiti P, Pandit JK. Polymeric nanoparticle system: A potential approach for ocular drug delivery. J Control Release 2009; 136: 2-13.
27. Gonzales-Mira E, Egea MA, Garcia ML, Souto EB. Design and ocular tolerance of flurbiprofen loaded ultrasound-engineered NLC. Colloids Surf. B. 2010; 81: 412-21.
28. Zlatkov A, Peikov P, Obreshkova D, Pencheva I. Spectral analyses methods for chemical compounds.1st ed, Plovdiv: Macros; 2010.
29. Singhvi G, Mahaveer S. In-vitro drug release characterization models. IJPSR. 2011; II(I): 77-84.
30. Collett J, Moreton R. Formulation of modified-release dosage forms. In, Aulton's Pharmaceutics. Edited by Aulton M, 3rd ed., Churchill Livingstone Elsivier; 2007.